

## ACCELERATED STRESS TESTING OF SiC PRESSURE TRANSDUCER

Constantin D. STANESCU , Cristiana VOICAN  
University "Politehnica of Bucharest"

[prof\\_cstanescu@yahoo.com](mailto:prof_cstanescu@yahoo.com) ; [voicancristiana@yahoo.com](mailto:voicancristiana@yahoo.com)

Keywords: Test, Temperature, Pressure Sensor, Silicon Carbide

**Abstract** .Preliminary accelerated stress tests (AST) have been performed on 6H-SiC pn-junction piezoresistive pressure transducers that were packaged by Microelectromechanical Systems Direct Chip Attach process for the purpose of evaluating their long-term operational stability and reliability under cyclic pressure and temperature. Finite element analysis (FEA) was used to understand the stress distribution at critical sensor/Aluminum nitride (AlN) header and AlN header/Kovar interfaces and to develop design strategies that minimize the thermomechanical stresses.

### 1. Introduction

There is a growing demand for pressure transducers that can operate reliably at temperatures ranging between 300 and 600°C. Pressure monitoring during deep well drilling and combustion in aeronautical and automobile engines require pressure transducers that can operate in this range of temperature [2]. There is also a growing demand for improved fuel efficiency in jet engines and automobiles as well as the reduction of undesirable emission of hydrocarbons and other combustion by-products such as NO<sub>x</sub> and CO [6]. However, it has remained a challenge to apply conventional semiconductor sensing devices because they are limited to operating temperatures less than 300°C due to the limitations imposed by their material properties, packaging technology, and design constraints. In cases where they are utilized at higher temperature, extensive and expensive packaging methods such as plumbing for water cooling are adopted. Sensor on insulator (SOI) technology has long been adopted to further extend the operational capability of pressure sensor to temperatures beyond 300°C [7]. While the SOI based sensors can be utilized for short duration instrumentation, their long term stability and reliability remain a challenge. Silicon carbide (SiC) has long been viewed as a potentially useful semiconductor for high temperature applications. SiC-based sensors have been demonstrated to operate at temperatures up to 600°C [1],[10], thereby offering promise of direct insertion into the high temperature environment without the need for cooling. However, the absence of reliable packaging methodologies for such extreme temperatures has largely prevented the application of SiC sensors. Devices capable of functioning in these harsh environments need the appropriate package to sustain operation throughout their operational life.

The identified failure mechanism is associated with the changes in resistance at the metallurgical junction between sensor and the wire bonds due to reaction kinetics that eventually weaken the bond [4]. Another prominent failure mechanism is the fatigue induced sensor cracking due to the thermomechanical stress between the sensor and the package components as a result of mismatches in the CTEs [8].

## 2. High Temperature Microsystems Packaging Issues

A survey of current packaging materials suggests that AlN is an ideal candidate for packaging SiC-devices for high-temperature (600°C) applications [9]. Some of the important advantages of AlN include high thermal conductivity ( $200 \text{ W}\cdot\text{m}^{-1}\cdot\text{K}^{-1}$ ), which decreases only slightly with increasing temperature; a CTE ( $4.1 \times 10^{-6} \text{ }^\circ\text{C}^{-1}$ ) that closely matches that of SiC ( $3.7 \times 10^{-6} \text{ }^\circ\text{C}^{-1}$ ), which minimizes the thermal stresses; good thermal shock resistance and environment stability at high temperatures; non-toxicity (unlike beryllia); high electrical resistivity; high mechanical strength; and chemical inertness at high temperatures.

Wire bonds are known to be the weakest links in a package that operates at high temperatures. The wires can fail by creep deformation at high temperatures. They can form unwanted intermetallics with the bond pad materials thereby weakening the wire bond interface.

## 3. Stress Analysis of the Package

In earlier works, more attention was focused on proof of concept demonstration of SiC pressure sensor operation at 600°C than on the effect of thermomechanical stress and its impact on mechanical and electrical sensor functionality and long-term reliability [1],[10]. While the first generation high temperature MEMS-DCA offered the promise of supporting sensor operation at 600°C and beyond, it was still hindered by the undesirable thermomechanical coupling between sensor and package components [10].

A second generation MEMS-DCA packaging as shown in cross section in Figure 1 was developed and used for packaging the SiC sensors reported in this paper [9]. The cross section depicts the primary components of the transducer and the several unique characteristics that combine to provide its robustness. The AlN is selected because its coefficient of thermal expansion (CTE),  $\alpha_{\text{AlN}} = 4.1 \text{ ppm}/^\circ\text{C}$  matches closely to that of SiC of  $\alpha_{\text{SiC}} = 3.7 \text{ ppm}/^\circ\text{C}$ . The CTE of the specially developed sealing glass also matches very close to that of SiC. The SiC sensor is housed in an AlN header and sealed with the glass to achieve a leak rate of better than  $10^{-7} \text{ l-atm}\cdot\text{s}^{-1} \text{ He}$ . When the sensor is placed on the circular cavity of the AlN receptacle, as shown in Figure 1, only the sensor's circular diaphragm is free to deflect in and out of the reference cavity. The sealing glass

is applied into the narrow gap ( $< 100 \mu\text{m}$ ) between the SiC sensor and AlN. The bond pads of the sensor align precisely with the holes in the AlN so that the wires that are inserted in these holes intimately contact the bond pads.

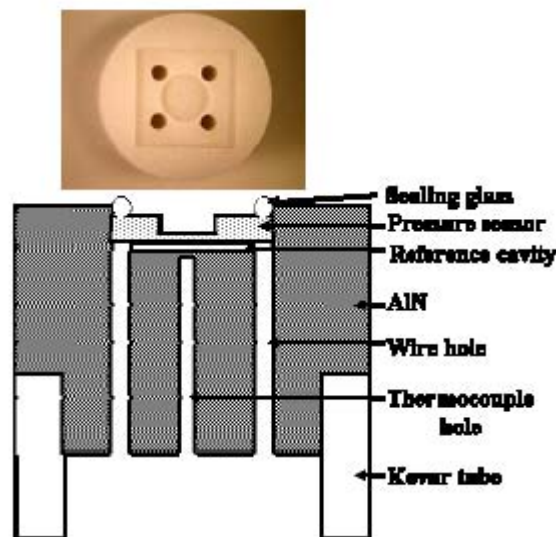


**Figure 1: Cross sectional and top views of the MEMS-DCA depicting unique advantages and novelty: direct wire contact eliminates wire bonding; higher density chip count on wafer; thermomechanical stress de-coupling of sensor from metal tube minimizes instability; thermocouple access provides for temperature measurement for compensation and calibration purposes.**

The stresses brought about by thermal cycling during service can induce fatigue at several critical areas of the system such as glass sealing/sensor and sensor/AlN interfaces. Therefore, to optimize the new package design concept, a non-linear finite element analysis (FEA) was conducted to establish the influence of the length of AlN cylinder on the stresses and deformation developing near the braze and the sensor surface. All parts of the assembly are modeled utilizing ANSYS SOLID45 eight node brick elements [5]. The contact between AlN cylinder and the bottom of the SiC is modeled by employing CONTA173 and TARGE170 elements. The non-linear solution procedure involves a two-step temperature loading. The non-linearity arises from the presence of the contact surface between the chip and the cylinder. By taking advantage of the symmetry of the structure as shown in Figure 2a, a quarter of the assembly was modeled. Consequently, the symmetry displacement boundary conditions were imposed to the appropriate sides of the components.

The results are depicted in terms of first principal and equivalent stress distributions near the AlN/Kovar braze joint and the AlN/SiC interface. In the FEA, the thermal loading applied in two steps begins with  $850^{\circ}\text{C}$ , the temperature at which the AlN is brazed to the Kovar tube, then reduces to  $650^{\circ}\text{C}$ , the temperature at which the glass is applied to the SiC sensor, and finally to  $25^{\circ}\text{C}$ . The distribution of the first principal and equivalent stresses in the layer of the SiC elements that is in contact with AlN cylinder is shown in Figures 2b and 2c, respectively. By varying the length to the AlN cylinder, the maximum stress

values seen at the edge of the SiC sensor remained unchanged at about 400 MPa (principal) and 652 MPa (equivalent).

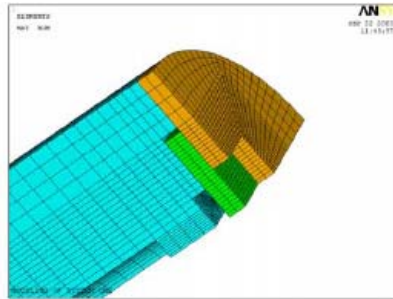


**Figure 2a:** Quarter symmetry model of the MEMS-DCA used for the analysis depicts the SiC chip sandwiched between the glass layer and the AlN cylinder.

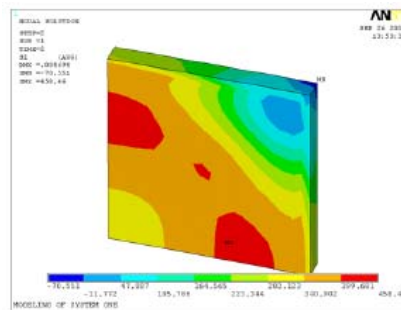


**Figure 2b:** The distribution of the first principal stress (MPa) in the layer of SiC elements that is in contact with AlN cylinder (AlN header – 25.4 mm).

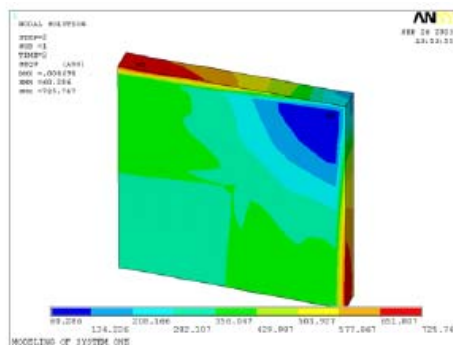


**Figure 2c:** The distribution of the equivalent stress (MPa) in the layer of SiC elements that is in contact with AlN cylinder (AlN header – 25.4 mm).

The gap, penetration, and pressure arising from the contact between AlN cylinder and SiC chip are presented hereafter. Figure 3a shows the modeled cavity surface along which the AlN cylinder is in contact with the SiC chip and is used for further reference. The distribution of the pressure arising from the contact between the AlN cylinder and SiC chip is shown in Figure 3b. As expected, the maximum contact pressure develops near the middle of the SiC

chip sides. In the broader context of the analysis, no considerable variation of the pressure is observed because of the different lengths of the AlN cylinder. The influence of the AlN cylinder length on the values of these stresses was found to be negligible.

In the transducers under discussion, the bridge circuit is asymmetric. Therefore, in a closed bridge condition, the output is obtained as:

$$V_{oz} = V_{in} \frac{1}{2} \left( \frac{R_2 - R_1}{R_1 + R_2} + \frac{R_4 - R_3}{R_3 + R_4} \right) \quad (1)$$

and the output resistance is resolved to be

$$R_o = \left( \frac{(R_2 + R_3)(R_1 + R_4)}{R_1 + R_2 + R_3 + R_4} \right) \quad (2)$$

Due to asymmetry, the bridge output,  $V_{oz}$ , under unstrained condition is non-zero. When pressure is applied to the diaphragm, each resistor experiences a strain that corresponds to the applied pressure. The relative change in each resistor element due to strain is generally expressed as:

$$\Delta R = R \varepsilon G \quad (3)$$

where  $G$  represents the gauge factor (strain sensitivity factor),  $\varepsilon$  is the strain corresponding to the pressure applied. The TCR of a resistor, denoted as  $\beta$  (ppm/°C), determines the resistor value at given temperature. This can be expressed as:

$$R_T = R_o (1 + \beta \Delta T) \quad (4)$$

where  $R_T$  ( $\Omega$ ) is the resistance at temperature,  $R_o$  is the resistance at room temperature, and  $\Delta T$  ( $^{\circ}\text{C}$ ) is the change in temperature from the reference temperature (usually room temperature). The temperature effect of the gauge factor, (strain sensitivity) is expressed as:

$$G_T = G_o (1 + \gamma \Delta T) \quad (5)$$

where  $\gamma$  is the temperature coefficient of gauge factor (ppm/°C) [(i.e. temperature coefficient of sensitivity (TCS)],  $G_T$  is the gauge factor at temperature and  $G_o$  is the gauge factor at room temperature.

### 3. Conclusion

The AST performed in this work represents the first effort to systematically measure and develop reliability criteria of single crystal pressure transducers targeted for long duration use at temperatures above the capability of silicon-based MEMS devices. FEA was used to optimize the MEMS-DCA package design, thus allowing for a successful de-coupling of the thermomechanical stress from high CTE package components to the sensors. We have established

benchmark reliability criteria for SiC pressure transducers for 300°C applications on the basis of the thermal stability of critical operational parameters. From this reliability evaluation, we have validated the stability and reliability of fully packaged 6H-SiC pressure sensors for over 130 hours operation at 300°C.

#### References

- [1] Alex A. Ned, Robert S. Okojie, and Anthony D. Kurtz, "6H-SiC Pressure Sensor Operation at 600°C," Trans. 4<sup>th</sup> Intl. High Temp. Elect. Conf., p. 257-260, 1998.
- [2] Alexandar's Gas and Oil Connections, News and Trends: North America, vol. 8, Issue 13, 2003.
- [3] ANSYS, Inc. Global Headquarters, Southpointe 275 Technology Drive, Canonsburg, PA 15317.
- [4] Chidambaram N.V., Proceedings 41<sup>st</sup> Electronic Components and Technology Conference, May 11-16, p. 877 – 882, 1991.
- [5] Ender Savrun, and Wayne R. Johnson "Aluminum Nitride Packages for High-Power, High-Temperature Electronics," Sienna Technical Report No. 982, NASA Contract No. NAS3-99046, 1999.
- [6] International Civil Aviation Organization Standards: Annex 16 - Environmental Protection, Volume II - Aircraft Engine Emissions, 1999
- [7] J. von Berg, Ziermann R., Reichert W., Obermeier E., . Eickhoff M, Krotz G., Thoma U., Cavalloni C., and Nendza J.P., 4<sup>th</sup> International High Temperature Electronics Conference, p. 45 – 249, 1998.
- [8] Michaelides S., Sitaraman S.K., IEEE Transactions on Advanced Packaging, Vol. 22, Issue: 4 , p.:602 – 613, 1999.
- [9] Robert S. Okojie, Patent pending
- [10] Robert S. Okojie, Glenn M. Beheim, George J. Saad, and Ender Savrun, "Characteristics of a Hermetic 6H-SiC Pressure Sensor at 600°C," Proc. 39<sup>th</sup> AIAA Mtg., Paper No. 2001-4652, 2001